



HAL
open science

A practical guide for synthetic fNIRS data generation

Jessica Gemignani, Judit Gervain

► **To cite this version:**

Jessica Gemignani, Judit Gervain. A practical guide for synthetic fNIRS data generation. 2021 43rd Annual International Conference of the IEEE Engineering in Medicine & Biology Society (EMBC), Nov 2021, Mexico, France. pp.828-831, 10.1109/EMBC46164.2021.9631014 . hal-03805187

HAL Id: hal-03805187

<https://hal.science/hal-03805187v1>

Submitted on 7 Oct 2022

HAL is a multi-disciplinary open access archive for the deposit and dissemination of scientific research documents, whether they are published or not. The documents may come from teaching and research institutions in France or abroad, or from public or private research centers.

L'archive ouverte pluridisciplinaire **HAL**, est destinée au dépôt et à la diffusion de documents scientifiques de niveau recherche, publiés ou non, émanant des établissements d'enseignement et de recherche français ou étrangers, des laboratoires publics ou privés.

A practical guide for synthetic fNIRS data generation

Jessica Gemignani^{1,*}, Judit Gervain^{1,2}

Abstract— The use of a large and diversified ground-truth synthetic fNIRS dataset enables researchers to objectively validate and compare data analysis procedures. In this work, we describe each step of the synthetic data generation workflow and we provide tools to generate the dataset.

I. INTRODUCTION

Functional Near Infrared Spectroscopy (fNIRS) is a non-invasive neuroimaging technique based on the measurement of the optical absorption of cerebral blood [1]. Thanks to the different absorption spectra of oxygenated and deoxygenated hemoglobin (HbO and HbR, respectively) in the near-infrared region of the electromagnetic spectrum (650–900 nm), fNIRS measures the relative changes of oxygenation and blood perfusion in the human brain at rest or in response to a specific task.

Its use in research has greatly increased over the last two decades [2] and so has the diversity in methodological practices. A large heterogeneity in experimental approaches and data analysis methods inevitably poses a challenge to the comparability and replicability of studies [3], which is why the fNIRS community is currently dedicating considerable effort to the systematic validation and standardization of practices for each aspect of fNIRS research, by comparing different hardware performances [4],[5], pre-processing methods [6]–[8] and techniques for the statistical analysis [9],[10], just to name a few, with the ultimate goal of establishing common, standardized and well-reproducible practices [11].

For the validation and comparison of different data analysis practices, synthetically generated and systematically parametrized ground-truth datasets are necessary, as they allow researchers full control over the metric(s) under investigation and provide insight into how data characteristics interact with analysis parameters, e.g., a given analysis pipeline, the choice of filtering or artifact rejection etc.

This paper offers a step-by-step illustration of the procedure followed for generating the synthetic fNIRS dataset employed in Gemignani et al. (2018) [12] and Gemignani and Gervain (2021) [8], and provides publicly available code to reproduce it and synthesize ground-through datasets with fully controllable parameters.

II. METHODS

Synthetic data was generated using tools available in the *Brain AnalyzIR Toolbox* for Matlab [13].

A. Experimental design and optode arrangement

As a first step, an experimental design needs to be identified, according to which hemodynamic responses will be placed along the timeseries.

The vast majority of fNIRS paradigms fall into one of the following categories: block design, event-related design and resting-state paradigms; for both event-related and block-paradigms, features of the design include: type of stimuli, number of conditions, number of trials per condition, trial order, trial duration and the duration of the inter-trial interval [11].

In this work, synthetic data was generated using the experimental design in Gervain et al. (2012) [14]. In that study, NIRS was acquired in 22 newborns using a montage with 24 channels.

We thus generated a synthetic dataset with 22 “participants”, each with 24 time series corresponding to the 24 channels. Like in the original study, the time series comprised two conditions, with 14 trials per condition, each lasting approximately 18 seconds, and spaced at time intervals of varying duration between 25 and 35 seconds.

B. Baseline noise

Physiological components of the signal, such as cardiac, respiratory and blood pressure changes, are typically much slower than the sampling rate of an fNIRS system [10], which is the reason why noise in fNIRS data has a colored structure and serial correlations: data points are not independent of their neighborings. In particular, two datapoints sampled 20 s apart still share 20% of the information, and, in case of 10 Hz data, it is necessary to apply a whitening filter of order 33 to achieve complete whitening of the noise (i.e., have completely independent neighboring samples), as demonstrated in [10].

To account for this, in generating synthetic data, baseline noise was produced by first generating white noise, then imposing temporal correlation on it by employing an autoregressive model of order 30.

This was achieved by modeling each fNIRS timeseries as

$$Y_t = \sum_{i=1}^p \varphi_i Y_{t-i} + \varepsilon_t$$

where $\varphi_1, \dots, \varphi_p$ are the randomly generated parameters of the model and ε_t is the noise [9].

¹ University of Padova, Department of Developmental Psychology and Socialization, Via Venezia 8, 35131 Padova, Italy

² University of Paris, Integrative Neuroscience and Cognition Center, Rue des Saints Peres 45, 75006 Paris, France

* Corresponding author (jessica.gemignani@unipd.it)

Besides presenting temporal correlation, real fNIRS data is also not independent across channels [10]; the spatial covariance existing between channels has an impact on the assumptions of the group-level statistical analysis. Since this relationship is not within the scope of this work, the specific dataset presented here was generated with no spatial correlation. However, synthetic datasets destined to test spatial hypotheses or different statistical analyses for fNIRS data should take spatial correlations into account.

After generating the temporally correlated baseline signal, physiological components were included. The temporal variation of these systemic signals can be as large as 10% [15]. Therefore, to simulate the contribution of heart rate, respiration and Mayer waves, the signal amplitude was increased by a factor ranging between 0.01 and 0.03 mM x mm (i.e., about 3-10% of the total signal change), at frequencies typical of the infant HRF: 1.5 ± 0.2 Hz, 0.25 ± 0.05 Hz and 0.1 ± 0.02 Hz, respectively.

C. Hemodynamic activity

The hemodynamic response (HRF) has been shown to vary in latency, amplitude and shape, both across individuals for the same region and across brain areas for the same individual [16].

Therefore, a realistic synthetic dataset should include responses of various sizes and/or shapes, depending on the goal of the study.

In this work, we included HRFs with amplitudes typical of infant fNIRS data [17], namely ranging between 0.1 and 0.35 mM-mm for HbO and between -0.05 and -0.175 mM-mm for HbR, and characterized by an onset-to-peak time of 6 seconds and an undershoot of 16 s after onset. HRFs were modelled with two gamma functions, for the peak and the undershoot, respectively. They were added to 12 channels, i.e. 50% of all channels, which are referred to as “active channels”.

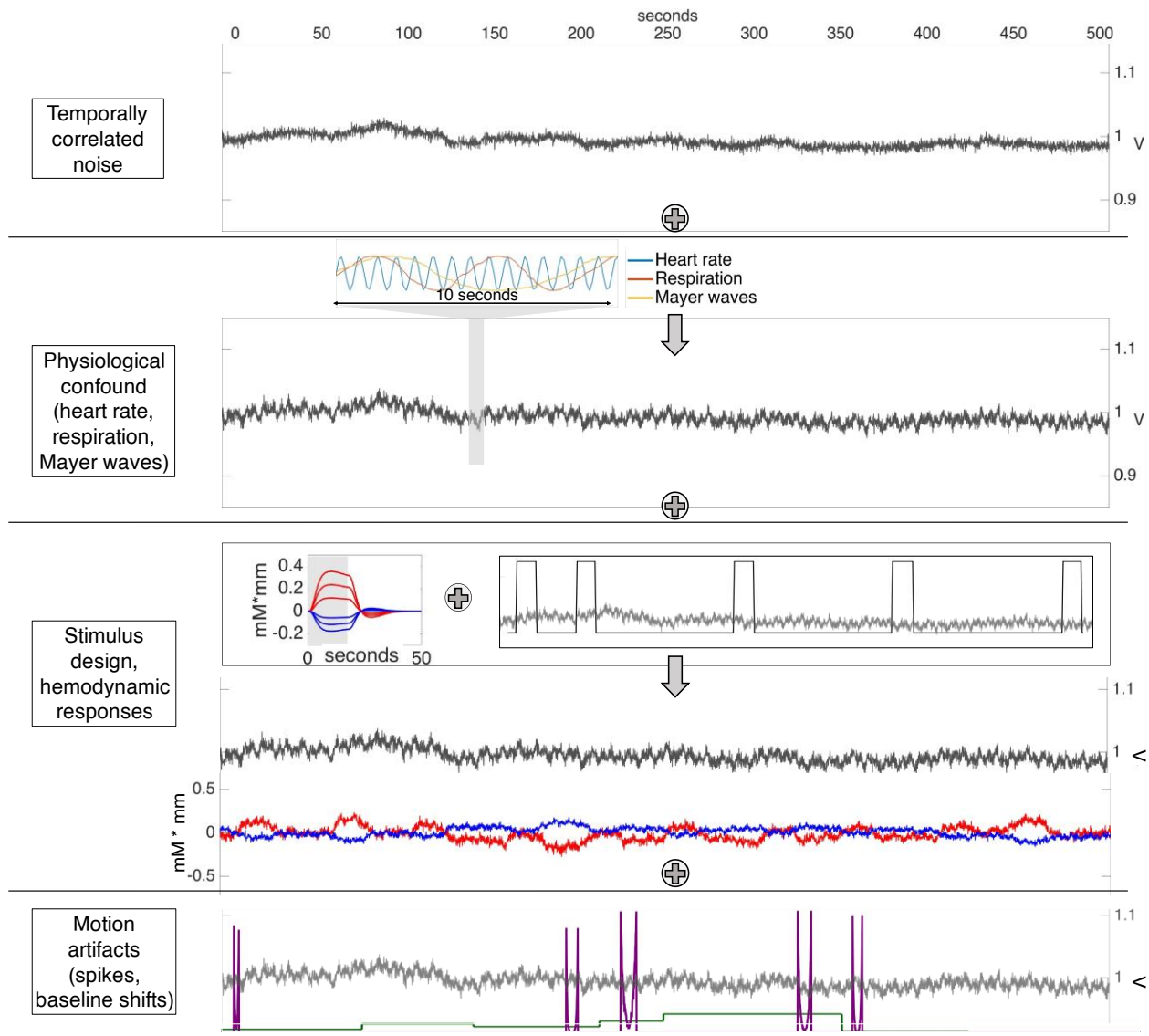


Figure 1: Procedure employed to produce the synthetic dataset.

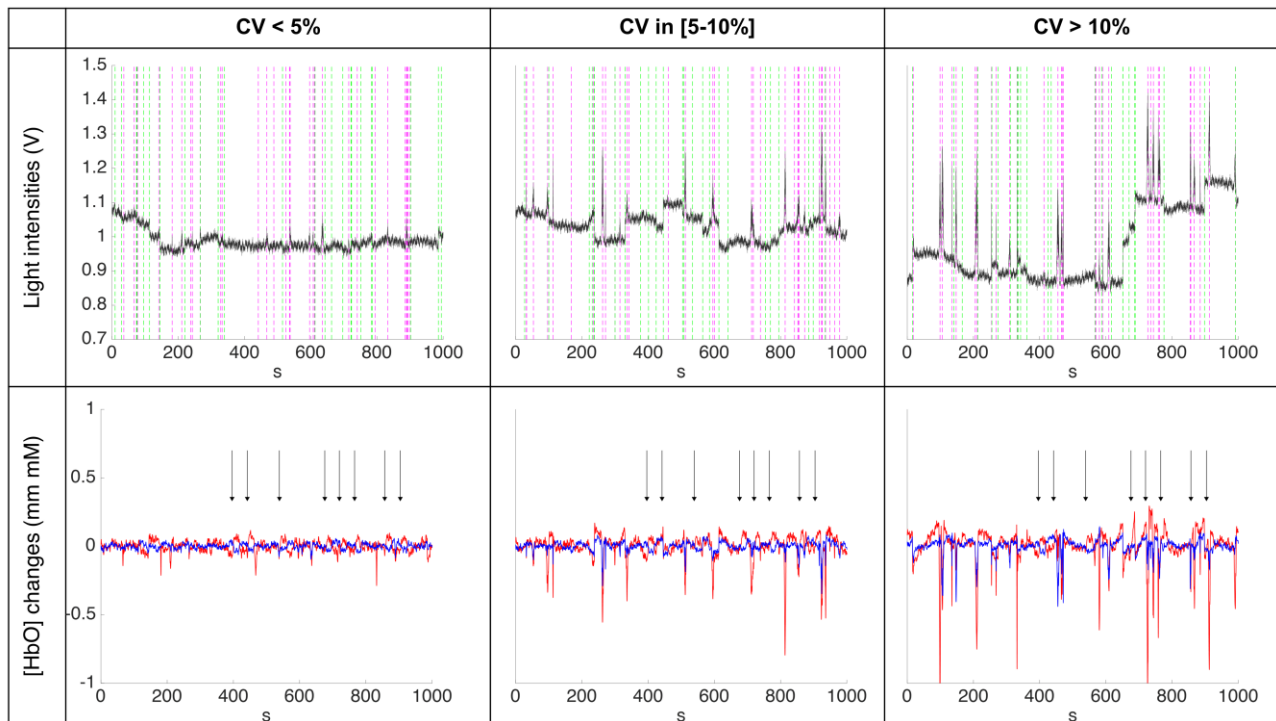


Figure 2: Examples of simulated data (upper row: light intensities, lower row: corresponding concentration changes); the three timeseries share the same baseline and physiological noise, but are characterized by increasing amplitude and frequency of spikes and shift artifacts, thus resulting in having different levels of noise, measured in terms of coefficient of variation (CV, standard deviation of the timeseries divided by its mean value)

D. Motion artifacts

Motion artifacts are the result of a temporary loss of optical coupling due to the displacement of the optodes during data acquisition.

Preventing their occurrence during the experiment, or at least mitigating their amplitude, is becoming increasingly feasible, thanks to steady improvements in fNIRS headgears [18]; nevertheless, it remains particularly challenging with non-compliant participants, like awake infants, since they cannot be instructed to stay motionless. Therefore, motion artifacts will appear in the timetraces, in the form of sudden spikes or shifts in baseline level.

It is particularly interesting to add motion artifacts to synthetic data, in order to evaluate how the metrics of interest change as the frequency and amplitude of artifacts increases (e.g. in [6]).

In our work, motion artifacts were added after the functional activity was included to specifically assess how they impair its recovery.

Spikes were modelled as a sudden change of voltage ranging between 0.1 and 2 V, while baseline shift artifacts were modelled as a random positive or negative change of voltage, also ranging between 0.1 and 2 V.

III. RESULTS

When generating a synthetic dataset, it is of crucial importance to be able to identify how factors under investigation (e.g. a given analysis method) interact with data characteristics. Taking a parametrized, systematic

approach is crucial: one dataset should only differ from the other along a single dimension, like spike amplitude or HRF size. This method therefore allows the user to systematically vary amplitudes and timing of the HRF and of the motion artifacts, allowing to precisely disentangle the effect of each variable on the resulting metric:

Figure 2 shows a resting state dataset with three different HRFs superimposed on it, characterized by the same HRF amplitude (0.07 mm x mM for this specific timetrace) but three different levels of noise, measured in terms of coefficient of variation of the time series.

IV. DISCUSSION

In this work, we describe in detail each step of a workflow that generates synthetic fNIRS data and provide the code to generate datasets. Adding HRFs and motion artifacts of increasing intensity and frequency reveals how these aspects impact analysis and how they interact with factors of interest (for example, different analysis methods may perform differently under different conditions of artifacts and/or HRF amplitudes).

The specific dataset generated here displays characteristics that make it similar to real infant data: this way, 22 “participants” were simulated, each with 20 different settings in terms of HRFs and motion artifacts; in [8], this allowed to compare six different pipelines and investigate their efficacy under different conditions of noise.

The procedure described is entirely flexible and it is possible to finely tune each parameter: duration of initial resting state; frequency ranges of physiological components and

corresponding amplitude changes; frequency of occurrence and amplitude of motion artifacts; amplitude of HRFs and distribution across channels.

The use of fully controlled synthetic datasets will help fNIRS researchers compare and objectively validate analysis methods, and ultimately design robust and reproducible analysis procedures.

APPENDIX

The code that reproduces the steps here described is available at <https://github.com/JessicaGem/nirs-resources>, file: syntheticfNIRS.m

ACKNOWLEDGMENT

This work was supported by the ERC Consolidator Grant “BabyRhythm 773202” awarded to Judit Gervain.

REFERENCES

- [1] M. Ferrari and V. Quaresima, “A brief review on the history of human functional near-infrared spectroscopy (fNIRS) development and fields of application,” *Neuroimage*, vol. 63, no. 2, pp. 921–935, 2012.
- [2] D. A. Boas, C. E. Elwell, M. Ferrari, and G. Taga, “Twenty years of functional near-infrared spectroscopy: Introduction for the special issue,” *NeuroImage*, vol. 85, Neuroimage, pp. 1–5, 15-Jan-2014.
- [3] A. Bizzego, J. P. M. Balagtas, and G. Esposito, “Commentary: Current Status and Issues Regarding Pre-processing of fNIRS Neuroimaging Data: An Investigation of Diverse Signal Filtering Methods Within a General Linear Model Framework,” *Frontiers in Human Neuroscience*, vol. 14, Frontiers Media S.A., p. 505, 14-Jul-2020.
- [4] A. Pifferi *et al.*, “Mechanically switchable solid inhomogeneous phantom for performance tests in diffuse imaging and spectroscopy,” *J. Biomed. Opt.*, vol. 20, no. 12, p. 121304, Jul. 2015.
- [5] S. R. P. K. Lanka *et al.*, “A multi-laboratory comparison of photon migration instruments and their performances: the BitMap exercise,” in *Optical Tomography and Spectroscopy of Tissue XIV*, 2021, vol. 11639, p. 11.
- [6] R. Di Lorenzo *et al.*, “Recommendations for motion correction of infant fNIRS data applicable to multiple data sets and acquisition systems,” *Neuroimage*, vol. 200, no. April, pp. 511–527, 2019.
- [7] P. Pinti, F. Scholkmann, A. Hamilton, P. Burgess, and I. Tachtsidis, “Current Status and Issues Regarding Pre-processing of fNIRS Neuroimaging Data: An Investigation of Diverse Signal Filtering Methods Within a General Linear Model Framework,” *Front. Hum. Neurosci.*, vol. 12, no. January, pp. 1–21, 2019.
- [8] J. Gemignani and J. Gervain, “Comparing different pre-processing routines for infant fNIRS data,” *Dev. Cogn. Neurosci.*, vol. 48, no. July 2020, p. 100943, 2021.
- [9] J. W. Barker, A. Aarabi, and T. J. Huppert, “Autoregressive model based algorithm for correcting motion and serially correlated errors in fNIRS,” *Biomed. Opt. Express*, vol. 4, no. 8, p. 1366, Aug. 2013.
- [10] T. J. Huppert, “Commentary on the statistical properties of noise and its implication on general linear models in functional near-infrared spectroscopy,” *Neurophotonics*, vol. 3, no. 1, p. 010401, 2016.
- [11] M. A. Yücel *et al.*, “Best practices for fNIRS publications,” *Neurophotonics*, vol. 8, no. 01, pp. 1–34, Jan. 2021.
- [12] J. Gemignani, E. Middell, R. L. Barbour, H. L. Graber, and B. Blankertz, “Improving the analysis of near-infrared spectroscopy data with multivariate classification of hemodynamic patterns: a theoretical formulation and validation,” *J. Neural Eng.*, vol. 15, no. 4, p. 045001, Aug. 2018.
- [13] H. Santosa, X. Zhai, F. Fishburn, and T. Huppert, “The NIRS Brain AnalyzIR Toolbox,” *Algorithms*, vol. 11, no. 5, p. 73, May 2018.
- [14] J. Gervain, I. Berent, and J. F. Werker, “Binding at birth: The newborn brain detects identity relations and sequential position in speech,” *J. Cogn. Neurosci.*, vol. 24, no. 3, pp. 564–574, 2012.
- [15] D. A. Boas, A. M. Dale, and M. A. Franceschini, “Diffuse optical imaging of brain activation: Approaches to optimizing image sensitivity, resolution, and accuracy,” in *NeuroImage*, 2004.
- [16] F. M. Miezin, L. Maccotta, J. M. Ollinger, S. E. Petersen, and R. L. Buckner, “Characterizing the hemodynamic response: Effects of presentation rate, sampling procedure, and the possibility of ordering brain activity based on relative timing,” *Neuroimage*, vol. 11, no. 6 I, pp. 735–759, 2000.
- [17] C. Issard and J. Gervain, “Variability of the hemodynamic response in infants: Influence of experimental design and stimulus complexity,” *Dev. Cogn. Neurosci.*, vol. 33, no. January, pp. 182–193, 2018.
- [18] J. Gervain *et al.*, “Near-infrared spectroscopy: A report from the McDonnell infant methodology consortium,” *Dev. Cogn. Neurosci.*, vol. 1, no. 1, pp. 22–46, 2011.